Photorefractive Effects and Structure/Property Correlation of Oligothiophenes Functionalized with Nonlinear Optical Chromophores

Man-Kit Ng, Liming Wang, and Luping Yu*

Department of Chemistry and The James Franck Institute, The University of Chicago, 5735 South Ellis Avenue, Chicago, Illinois 60637

Received March 16, 2000. Revised Manuscript Received July 11, 2000

A homologous series of fully functionalized regioregular oligo(3-alkylthiophenes) **10**−**12** bearing a nonlinear optical (NLO) chromophore was synthesized. An alternating sequence of bromination and Stille cross-coupling reactions was developed for the synthesis of these oligomers and regiochemically pure, trimethylsilyl-substituted bithiophene organostannane **2c** was utilized as the building block. The resulting materials were shown to form stable amorphous films exhibiting a large photorefractive (PR) effect. Two-beam coupling and degenerate four-wave mixing experiments demonstrate large optical net gain and high diffraction efficiency. It was also found that the PR performance of these oligomers depends on the π-conjugation chain length with an optimized conjugation length.

Introduction

A photorefractive (PR) material possesses the ability to modulate its index of refraction under inhomogeneous illumination by low-intensity light. This property can find potential applications in such areas as real-time information processing, optical data storage, and phase conjugation.[1] In a PR material, two types of physical properties must exist simultaneously: photoconductivity and electrooptic response. The refractive index modulation arises from the linear electrooptic effect (Pockels effect) of the nonlinear optical (NLO) chromophore in response to the internal space-charge field within a photoconducting medium. Recently, significant effort has been devoted to the study of novel PR polymeric and oligomeric systems because of their good processibility, versatility for structural modifications, and low cost compared to their inorganic counterparts.[2−13] On the basis of our previous experience in the design of fully functionalized conjugated photorefractive polymers, we have described the PR properties of a multifunctional oligo(3-alkylthiophene) molecule containing a pendant NLO chromophore.[13] All the functionalities necessary to exhibit the PR effect exist in this simple molecular system. The conjugated oligothiophene backbone is photoconductive in the visible light region and plays the role of the photoconductive component, which in turn gives rise to a photoinduced space-charge field under inhomogeneous illumination. The pendant, covalently linked NLO chromophore is responsible for refractive index modulation. The reason to select oligothiophene (OT) is that we have developed an efficient synthetic approach to OT previously and these molecules possess high photoconductivity. Furthermore, OT molecules with long alkyl side chains are amorphous, a highly desirable feature in the practical applications of PR materials. It is observed that films made of this multifunctional, low-T_g oligothiophene-based material can be maintained in the amorphous state and without phase separation for an extended period of time.

However, there is only one compound that was studied and hardly any meaningful structure/property relationship was abstracted. As a continuation of our interest in improving the PR performance of this molecular system, it is important to gain a better understanding of the relationship between the PR properties and structural parameters such as the effect of the 3-alkyl chain substituents as well as the degree of conjugation of the oligothiophene-based system. We were therefore prompted to expand the scope of the methodologies available for constructing highly functionalized OT molecules[14−25] and to correlate the PR properties with the molecular structure of the OT

(1) Günter, P.; Huignard, J. P., Eds. *Photorefractive Materials and Their Applications*; Springer-Verlag: Berlin, 1988; Vol. 1.
(2) Moerner, W. E.; Silence, S. M. *Chem. Rev.* **1994**, *94*, 127.
(3) Moerner, W. E.; Grunnet-Jepsen, A.; Thompson, C. L. *Annu. Rev. Mater. Sci.* **1997**, *27*, 585.
(4) Meerholz, K. *Angew. Chem., Int. Ed. Engl.* **1997**, *36*, 945.
(5) Würthner, F.; Wortmann, R.; Matschiner, R.; Lukaszuk, K.; Meerholz, K.; DeNardin, Y.; Bittner, R.; Bräuchle, C.; Sens, R. *Angew. Chem., Int. Ed. Engl.* **1997**, *36*, 2765.
(6) Yu, L.; Chan, W. K.; Peng, Z.; Gharavi, A. *Acc. Chem. Res.* **1996**, *29*, 13.
(7) Wang, Q.; Wang, L.; Yu, L. *J. Am. Chem. Soc.* **1998**, *120*, 12860.
(8) Zhang, Y.; Burzynski, R.; Ghosal, S.; Casstevens, M. K. *Adv. Mater.* **1996**, *8*, 111.
(9) Meerholz, K.; Volodin, B. L.; Sandalphon; Kippelen, B.; Peyghambarian, N. *Nature* **1994**, *371*, 497.
(10) Kippelen, B.; Marder, S. R.; Hendrichy, E.; Maldonado, J. L.; Guillemet, G.; Volodin, B. L.; Steele, D. D.; Edami, Y.; Sandalphon; Yao, Y. J.; Wang, J. F.; Röchel, H.; Erskine, L.; Peyghambarian, N. *Science* **1998**, *279*, 54.
(11) Grunnet-Jepsen, A.; Thompson, C. L.; Moerner, W. E. *J. Opt. Soc. Am. B* **1998**, *15*, 905.
(12) Zhang, Y.; Wada, T.; Sasabe, H. *J. Mater. Chem.* **1998**, *8*, 809.
(13) Li, W.; Gharavi, A.; Wang, Q.; Yu, L. *Adv. Mater.* **1998**, *10*, 927.
(14) Briehn, C. A.; Kirschbaum, T.; Bäuerle, P. *J. Org. Chem.* **2000**, *65*, 352.
(15) Kirschbaum, T.; Azumi, R.; Mena-Osteritz, E.; Bäuerle, P. *New J. Chem.* **1999**, 241.

10.1021/cm000232x CCC: $19.00
Published on Web 08/31/2000

system. The synthesis of a series of doubly end-capped, regioregular head-to-tail coupled oligo(3-alkylthiophenes) bearing NLO chromophores is described. One of the structural features of these OT molecules is the presence of β-branched side chains on the 3-position of each of the constituting thiophene unit, resulting in a stereorandom mixture of stereoisomers. These stereoisomers help to lower T_g values of the resulting materials and prevent materials from crystallization. The materials can be solution-cast to provide transparent thick films with high optical quality without crystallization. Detailed physical studies revealed their interesting features and furnished with insightful structure/property correlation.

Experimental Section

Unless otherwise specified, all chemicals were purchased from commercial suppliers and used without further purification. All reactions were conducted under a nitrogen atmosphere unless otherwise specified. Tetrahydrofuran (THF) was distilled over sodium/benzophenone ketyl under a nitrogen atmosphere prior to use. ^{1}H NMR spectra were recorded at 400 or 500 MHz on Brüker DRX-400 or Brüker DRX-500 spectrometers, respectively. ^{13}C NMR spectra at 100 or 125 MHz were obtained on Brüker DRX-400 or DRX-500 spectrometers, respectively. $CDCl_3$ was used as the solvent to obtain all the ^{1}H and ^{13}C NMR spectra. ^{1}H chemical shift (δ) are reported in parts per million (ppm) downfield from tetramethylsilane. ^{13}C chemical shift (δ) are reported with the diagnostic 77.0 ppm $CDCl_3$ resonance as an internal reference. Differential scanning calorimetry was performed on a DSC-10 system (TA Instruments) under a nitrogen atmosphere at a heating rate of 10 °C min^{-1}. UV−vis spectra were taken on a Shimadzu UV-2401PC spectrophotometer. Cyclic voltammetry was performed on an EG&G Princeton Applied Research model 273 potentiostat/galvanostat controlled by EG&G M270 software. All electrochemical experiments were carried out in a three-electrode compartment cell (Bioanalytical Systems Inc.) equipped with a platinum disk as working electrode, a platinum wire as counterelectrode, and a $Ag/AgNO_3$ electrode as reference electrode. The supporting electrolyte used was tetrabutylammonium hexafluorophosphate (0.1 M in dichloromethane). The scan rate was adjusted to 100 mV s^{-1}. All potentials were calibrated with ferrocene/ferrocenium (Fc/Fc^+) couple after each experiment. All reported $E_{1/2}$ values are taken as the average of the anodic and cathodic peak potentials unless otherwise specified.[26,27] Mass spectrometry was provided by the Washington University Mass Spectrometry Resource (St. Louis, MO). Elemental analyses were performed by the Atlantic Microlab, Inc. (Norcross, GA).

The films for two-beam coupling and four-wave mixing experiments were prepared by sandwiching the materials between two indium−tin oxide (ITO) covered glass substrates. The thickness of the film was maintained at 127 μm with the help of a polyimide spacer. Two-beam coupling experiments were performed using a He−Ne laser (632.8 nm, 30 mW) as the light source. The *p*-polarized laser beam was split into two beams with equal intensity (0.83 W cm^{-2}), which were intersected in the film with an incident-crossing angle of 7.5° to generate the refractive index grating. The film normal was titled an angle of 53° with respect to the symmetric axis of the two writing beams to provide a nonzero projection of the grating wave vector along the poling axis. The transmitted intensities of the two beams were monitored by two calibrated diode detectors. The electric field-induced birefringence was measured by an ellipsometric method in a transmission mode.[28,29] The sample normal was titled at 45° with respect to the incident light. The polarization of the incident light was 45° with respect to the incident plane. A high DC voltage was applied to the film to align the NLO chromophore. The transmitted light after the analyzer was measured at different applied electric field. The field-induced optical birefringence Δn^{fi} was calculated from the intensity ratio of the transmitted light and the input light. Diffraction efficiency was measured by degenerate four-wave mixing (DFWM) experiment. In a DFWM experiment, two *s*-polarized laser beams (632.8 nm) of equal intensities intersected in the film to write the index grating, and a weak *p*-polarized beam (probe beam) counterpropagating to one of the writing beams was used to read the index grating formed in the material. The diffracted light intensity of the probe beam was detected by a photodiode and subsequently amplified with a lock-in amplifier. The diffraction efficiency, η, was calculated as the ratio of the intensities of the diffracted beam to the incident reading beam. All the measurements were automatically controlled by a computer.

Compounds **1a**,[30] **1b**,[31] **1c**,[23] **2d**,[20] 4-[*N*-hexyl-*N*-(6-hydroxyhexyl)amino]benzaldehyde,[32] 3-oxobenzo[*b*]thiophene-1,1-dioxide,[33] and 4-[(*tert*-butyldimethylsilyl)oxy]bromobenzene[34] were prepared according to literature procedures.

NLO Chromophore 7. A mixture of 4-[*N*-hexyl-*N*-(6-hydroxyhexyl)amino]benzaldehyde (0.252 g, 0.82 mmol) and 3-oxobenzo[*b*]thiophene-1,1-dioxide[33] (0.25 g, 0.82 mmol) in absolute ethanol (65 mL) was heated under reflux for 24 h. After being cooled to room temperature, the mixture was concentrated under reduced pressure and the residue was purified by flash chromatography on silica gel (hexanes/ethyl acetate = 1/1) to provide the chromophore **7** (0.212 g, 0.45 mmol, 55%). ^{1}H NMR (400 MHz, $CDCl_3$) δ 0.91 (t, J = 6.7 Hz, 3 H), 1.33−1.46 (m, 10 H), 1.57−1.68 (m, 6 H), 3.37−3.43 (m, 4 H), 3.67 (m, 2 H), 6.72 (d, J = 9.2 Hz, 2 H), 7.77 (ddd, J = 1.0, 7.5, and 7.5 Hz, 1 H), 7.85 (ddd, J = 1.1, 7.5, and 7.5 Hz, 1 H), 7.92 (s, 1 H), 8.02 (d, J = 9.2 Hz, 2 H), and 8.00−8.07 (m, 2 H); ^{13}C NMR (100 MHz, $CDCl_3$) δ 13.9, 22.5, 25.5, 26.6, 26.7, 27.2, 31.5, 32.5, 51.1, 51.3, 62.6, 111.9, 117.8, 120.9, 122.4, 124.1, 133.0, 133.6, 135.2, 137.6, 143.6, 144.9, 152.7, and 178.7; HRMS (FAB) *m/z* calcd for $C_{27}H_{35}O_4NS$ (MH^+) 470.2365, found 470.2376. Anal. Calcd for $C_{27}H_{35}O_4NS$: C, 69.05; H, 7.51. Found: C, 68.83; H, 7.58.

Fully Functionalized Compound 10. The Grignard reagent derived from a mixture of magnesium turnings (0.060 g, 2.464 mmol) and 4-[(*tert*-butyldimethylsilyl)oxy]bromobenzene (0.708 g, 2.464 mmol) in dry THF (15 mL) was cooled to 0 °C and quenched with excess tributyltin chloride. After being warmed to room temperature, the resulting clear solution was transferred via a double-tipped needle to a mixture of **5d** (2.81 g, 1.54 mmol) and $Pd(PPh_3)_4$ (0.053 g, 0.046 mmol) in toluene (20 mL). The resulting mixture was heated at 110−115 °C for 10 h. Upon cooling to room temperature, excess solvent was removed under reduced pressure and the residue was purified

(16) Malenfant, P. R. L.; Jayaraman, M.; Fréchet, J. M. J. *Chem. Mater.* **1999**, *11*, 3420.
(17) Malenfant, P. R. L.; Fréchet, J. M. J. *Chem. Commun.* **1998**, 2657.
(18) Bidan, G.; De Nicola, A.; Enée, V.; Guillerez, S. *Chem. Mater.* **1998**, *10*, 1052.
(19) Guillerez, S.; Bidan, G. *Synth. Met.* **1998**, *93*, 123.
(20) Li, W.; Maddux, T.; Yu, L. *Macromolecules* **1996**, *29*, 7329.
(21) Barbarella, G.; Zambianchi, M. *Tetrahedron* **1994**, *50*, 11249.
(22) Barbarella, G.; Bongini, A.; Zambianchi, M. *Macromolecules* **1994**, *27*, 3039.
(23) Tour, J. M.; Wu, R. *Macromolecules* **1992**, *25*, 1901.
(24) Tour, J. M. *Chem. Rev.* **1996**, *96*, 537.
(25) Roncali, J. *Chem. Rev.* **1997**, *97*, 173.
(26) Adams, R. N. *Electrochemistry at Solid Electrodes*; Marcel Dekker: New York, 1969; pp 143−162.
(27) Hamann, C. H.; Hamnett, A.; Vielstich, W. *Electrochemistry*; Wiley-VCH: Weinheim, Germany, 1998; pp 222−234.
(28) Teng, C. C.; Man, H. T. *Appl. Phys. Lett.* **1990**, *56*, 1734.
(29) Harding, G. F. In *Optical Properties of Polymers*; Meeten, G. H., Ed.; Elsevier Applied Science: New York, 1986; pp 72.
(30) Van Pham, C.; Mark, H. B., Jr.; Zimmer, H. *Synth. Commun.* **1986**, *16*, 689.
(31) Kellogg, R. M.; Schaap, A. P.; Harper, E. T.; Wynberg, H. *J. Org. Chem.* **1968**, *33*, 2902.
(32) Robello, D. R. *J. Polym. Sci., Polym. Chem.* **1990**, *28*, 1.
(33) Arndt, F.; Kirsch, A.; Nachtwey, P. *Chem. Ber.* **1926**, *59*, 1074.
(34) Guthikonda, R. N.; Cama, L. D.; Quesada, M.; Woods, M. F.; Salzmann, T. N.; Christensen, B. G. *J. Med. Chem.* **1987**, *30*, 871.

by flash chromatography on silica gel (hexanes/toluene = 80/1 gradient to 2/1) to afford the fully functionalized **10** (1.80 g, 0.92 mmol, 60%) as an amorphous red solid. ^{1}H NMR (500 MHz, $CDCl_3$) δ 0.24 (s, 6 H), 0.88−0.92 (m, 39 H), 1.00 (s, 9 H), 1.21−1.40 (m, 58 H), 1.55−1.71 (m, 12 H), 2.58 (d, J = 7.2 Hz, 2 H), 2.74 (d, J = 7.0 Hz, 10 H), 3.39−3.45 (m, 4 H), 4.36 (t, J = 6.5 Hz, 2 H), 6.74 (d, J = 9.2 Hz, 2 H), 6.88 (d, J = 8.5 Hz, 2 H), 6.95 (s, 2 H), 6.96 (s, 1 H), 6.97 (s, 1 H), 6.98 (s, 1 H), 7.24 (s, 1 H), 7.32 (d, J = 8.5 Hz, 2 H), 7.66 (d, J = 8.4 Hz, 2 H), 7.77 (dd, J = 7.5 and 7.6 Hz, 1 H), 7.84 (dd, J = 7.5 and 7.5 Hz, 1 H), 7.93 (s, 1 H), 8.02 (d, J = 9.2 Hz, 2 H), 8.02−8.07 (m, 2 H), and 8.04 (d, J = 8.4 Hz, 2 H); ^{13}C NMR (100 MHz, $CDCl_3$) δ −4.5, 10.7, 10.7, 14.0, 14.1, 14.1, 22.6, 23.0, 23.1, 25.6, 25.6, 25.7, 25.9, 26.6, 26.7, 27.3, 28.6, 28.7, 28.7, 31.5, 32.5, 33.5, 33.5, 33.7, 40.1, 40.4, 51.1, 51.3, 64.7, 111.9, 117.9, 120.0, 120.9, 122.6, 124.1, 125.0, 127.4, 128.1, 128.7, 129.3, 129.4, 129.5, 129.7, 130.2, 130.6, 131.2, 131.4, 131.6, 132.3, 133.0, 133.0, 133.1, 133.3, 133.4, 133.5, 135.2, 137.5, 137.6, 138.2, 138.5, 138.5, 138.8, 138.9, 139.0, 139.9, 143.7, 144.8, 152.6, 155.1, 166.2, and 178.6; MS (MALDI) m/z calcd for $C_{118}H_{165}O_6NS_7Si$ (M^+) 1944.0451, found 1945.25. Anal. Calcd for $C_{118}H_{165}O_6NS_7Si$: C, 72.83; H, 8.55. Found: C, 72.62; H, 8.82.

Fully Functionalized Compound 11. A mixture of **5d** (2.50 g, 1.37 mmol), organostannane **8b** (1.94 g, 2.19 mmol), and $Pd(PPh_3)_4$ (0.047 g, 0.041 mmol) in toluene (18 mL) was heated at 110−115 °C for 10 h. Upon cooling of the mixture to room temperature, excess solvent was removed under reduced pressure and the residue was purified by flash chromatography on silica gel (hexanes/toluene = 80/1 gradient to 2/1) to afford the fully functionalized **11** (2.05 g, 0.88 mmol, 64%) as an amorphous red solid. ^{1}H NMR (500 MHz, $CDCl_3$) δ 0.24 (s, 6 H), 0.86−0.90 (m, 51 H), 1.00 (s, 9 H), 1.21−1.43 (m, 74 H), 1.55−1.75 (m, 14 H), 2.58 (d, J = 7.1 Hz, 2 H), 2.74 (d, J = 7.0 Hz, 14 H), 3.39−3.45 (m, 4 H), 4.36 (t, J = 6.5 Hz, 2 H), 6.73 (d, J = 9.2 Hz, 2 H), 6.88 (d, J = 8.5 Hz, 2 H), 6.94 (s, 4 H), 6.96 (s, 1 H), 6.97 (s, 1 H), 6.98 (s, 1 H), 7.23 (s, 1 H), 7.32 (d, J = 8.5 Hz, 2 H), 7.66 (d, J = 8.5 Hz, 2 H), 7.77 (dd, J = 7.5 and 7.6 Hz, 1 H), 7.84 (dd, J = 7.5 and 7.5 Hz, 1 H), 7.92 (s, 1 H), 8.01−8.06 (m, 2 H), 8.02 (d, J = 9.2 Hz, 2 H), 8.04 (d, J = 8.4 Hz, 2 H); ^{13}C NMR (125 MHz, $CDCl_3$) δ −4.4, 10.7, 10.7, 13.6, 14.0, 14.1, 14.1, 14.1, 17.2, 17.5, 18.2, 22.6, 23.0, 23.1, 25.6, 25.7, 25.7, 25.9, 26.6, 26.7, 26.7, 26.8, 27.3, 27.3, 27.8, 28.2, 28.6, 28.7, 28.7, 31.5, 32.5, 32.6, 33.5, 33.6, 33.7, 40.2, 40.4, 51.2, 51.4, 64.7, 111.9, 118.0, 120.0, 120.9, 122.7, 124.2, 125.0, 127.5, 128.1, 128.8, 128.8, 129.3, 129.4, 129.4, 129.5, 129.5, 129.8, 130.2, 130.6, 131.1, 131.2, 131.2, 131.4, 131.6, 132.3, 133.0, 133.1, 133.1, 133.4, 133.5, 133.6, 135.2, 137.6, 137.6, 138.3, 138.5, 138.5, 138.9, 138.9, 139.0, 139.0, 139.0, 140.0, 143.7, 144.9, 152.6, 155.1, 166.2, and 178.7; MS (MALDI) m/z calcd for $C_{142}H_{201}O_6NS_9Si$ (M^+) 2332.2709, found 2332.18. Anal. Calcd for $C_{142}H_{201}O_6NS_9Si$: C, 73.05; H, 8.68. Found: C, 73.03; H, 8.57.

Fully Functionalized Compound 12. Following the general procedure described for **11**, a mixture of **5d** (2.8 g, 1.54 mmol), organostannane **9b** (3.14 g, 2.46 mmol), and $Pd(PPh_3)_4$ (0.053 g, 0.046 mmol) in toluene (18 mL) at 110−115 °C for 10 h provided the fully functionalized **12** (2.31 g, 0.85 mmol, 55%) as an amorphous red solid. ^{1}H NMR (500 MHz, $CDCl_3$) δ 0.23 (s, 6 H), 0.87−0.94 (m, 63 H), 1.01 (s, 9 H), 1.20−1.45 (m, 90 H), 1.56−1.70 (m, 16 H), 2.56 (d, J = 7.1 Hz, 2 H), 2.73 (d, J = 6.7 Hz, 18 H), 3.39−3.44 (m, 4 H), 4.36 (t, J = 6.5 Hz, 2 H), 6.73 (d, J = 9.1 Hz, 2 H), 6.87 (d, J = 8.5 Hz, 2 H), 6.94 (s, 7 H), 6.96 (s, 1 H), 6.97 (s, 1 H), 7.23 (s, 1 H), 7.31 (d, J = 8.5 Hz, 2 H), 7.66 (d, J = 8.4 Hz, 2 H), 7.77 (dd, J = 7.4 and 7.6 Hz, 1 H), 7.84 (dd, J = 7.4 and 7.6 Hz, 1 H), 7.92 (s, 1 H), 8.02 (d, J = 9.1 Hz, 2 H), 8.04 (d, J = 8.5 Hz, 2 H), 8.02−8.07 (m, 2 H); ^{13}C NMR (100 MHz, $CDCl_3$) δ −4.5, 10.7, 14.0, 14.0, 14.1, 22.6, 22.9, 23.1, 25.5, 25.6, 25.6, 25.7, 25.9, 26.6, 27.2, 28.6, 28.7,, 31.5, 32.5, 33.5, 33.5, 33.7, 40.1, 40.4, 51.1, 51.3, 64.7, 111.8, 117.9, 120.0, 120.8, 122.7, 124.1, 124.9, 127.4, 128.1, 128.7, 128.7, 129.3, 129.4, 129.5, 129.7, 130.1, 130.5, 131.0, 131.0, 131.1, 131.1, 131.3, 131.6, 132.3, 133.0, 133.0, 133.1, 133.4, 133.5, 135.1, 137.5, 137.5, 138.2, 138.4, 138.8, 138.9, 138.9, 139.9, 143.7, 144.7, 152.5, 155.1, 166.1, and 178.5; MS (MALDI) m/z calcd for $C_{166}H_{237}O_6NS_{11}Si$ (M^+) 2720.4968, found 2720.19. Anal. Calcd for $C_{166}H_{237}O_6NS_{11}Si$: C, 73.21; H, 8.77. Found: C, 72.92; H, 8.76.

Results and Discussion

Synthesis of Molecules. Because of their outstanding optical and electronic properties as well as their environmental stability, conjugated polythiophenes (PTs) have been widely researched in the past few decades. It is now well established that the high regioregularity of the adjacent thiophene units in poly(3-alkylthiophenes) substantially increases the conjugation length of the polymers due to minimization of steric interactions among the monomeric thiophene rings.[35] For instance, regioregular head-to-tail coupled PTs exhibit substantially higher electrical conductivities than that of the regiorandom analogues. Efficient methodologies for the preparation of highly regioregular head-to-tail coupled PTs have been developed.[19,36−38] We and others have recently documented the synthesis of regioregular head-to-tail coupled oligo(3-alkylthiophenes).[14−25] In the present work, both termini of the oligothiophene unit in the target molecules, **10**−**12**, were capped with functionalized phenyl groups, allowing for the introduction of a NLO chromophore by standard coupling methodology. The target molecules were synthesized via the assembly of two complementary oligothiophene units in a head-to-tail fashion through palladium-catalyzed cross-coupling reaction, the Stille coupling reaction.[39] This coupling reaction can tolerate a variety of functional groups as those in the NLO chromophore. To efficiently synthesize the OT series, functionalized bithiophenes were used as the building molecules. The key building block, 5-trimethylsilyl-3′,4-di(2″-ethylhexyl)-2,2′-bithiophene, **2a**, was prepared from the palladium-mediated Negishi cross-coupling[40] of 2-bromo-3-(2′-ethylhexyl)thiophene **1b** with the organozinc reagent derived from 2-trimethylsilyl-3-(2′-ethylhexyl)thiophene **1c** (Scheme 1). The trimethylsilyl group on the reactive 5-position of **2a** proves to be critical in achieving complete regiocontrol in the buildup of the regioregular OT series. It is noted that the building block **2a** was contaminated by 5−8% of the symmetrical 5,5′-bis-(trimethylsilyl)-4,4′-di(2″-ethylhexyl)-2,2′-bithiophene **2b**, due to homocoupling of the organometallic partner. No improvement was observed when the catalytic system was changed from $Pd(PPh_3)_4$ to $PdCl_2$(dppf) or $PdCl_2(PPh_3)_2/PPh_3$. However, this impurity will not interfere with the following reactions. Compound **2a** was readily lithiated and converted into organostannane **2c** (*n*-BuLi, TMEDA, THF; Bu_3SnCl, 0 °C). The organostannane **2c** was cross-coupled with methyl 4-iodobenzoate to provide bithiophene ester **3a** in 90% yield with >99% regiochemical purity as evidenced by ^{1}H NMR spectroscopy (Scheme 2). Compound **2b** was removed by silica gel chromatography after the coupling reaction. The ter-

(35) McCullough, R. D. *Adv. Mater.* **1998**, *10*, 93 and references therein.
(36) McCullough, R. D.; Lowe, R. D.; Jayaraman, M.; Anderson, D. L. *J. Org. Chem.* **1993**, *58*, 904.
(37) Chen, T.-A.; Wu, X.; Rieke, R. D. *J. Am. Chem. Soc.* **1995**, *117*, 233.
(38) Iraqi, A.; Barker, G. W. *J. Mater. Chem.* **1998**, *8*, 25.
(39) Stille, J. K. *Angew. Chem., Int. Ed. Engl.* **1986**, *25*, 508.
(40) Negishi, E. *Acc. Chem. Res.* **1982**, *15*, 340.

Scheme 1

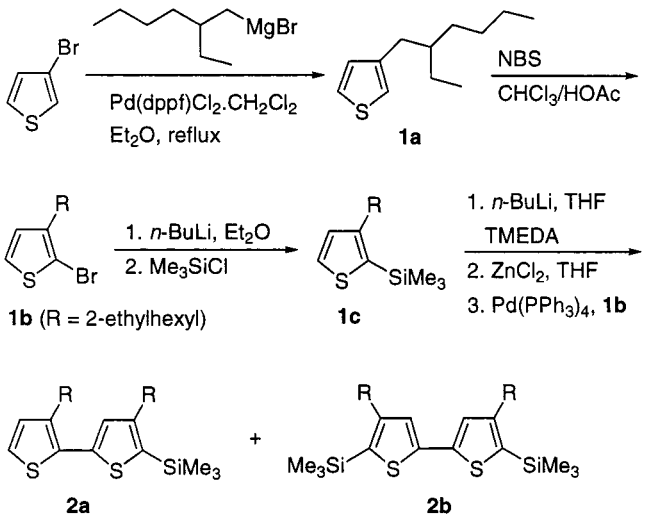

Scheme 2

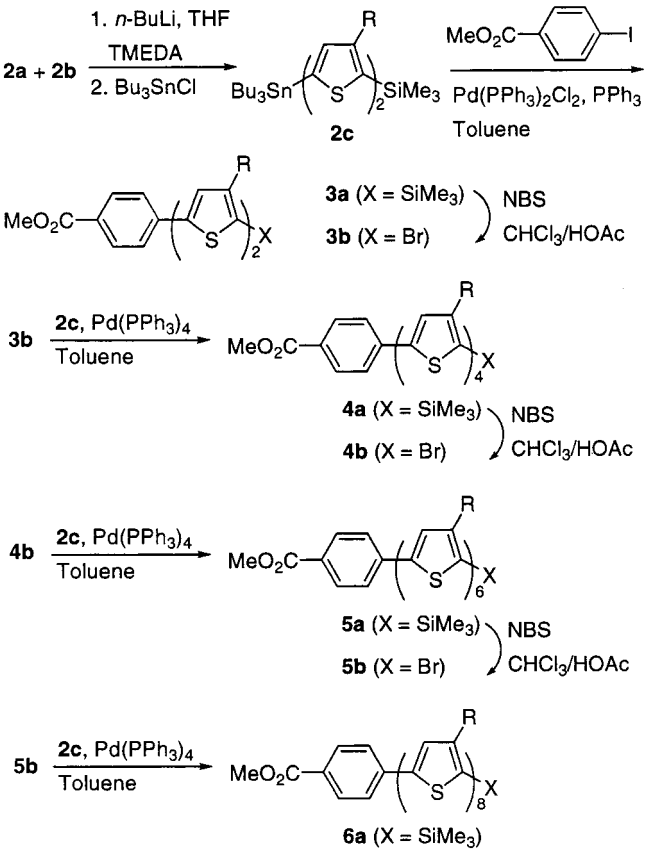

minal trimethylsilyl blocking group in the OT series was stable and no desilylation was observed during the usual workup and subsequent silica gel chromatographic purification. Because of the excellent stability toward base as well as the low cost and ease of installation of the trimethylsilyl group, no other blocking group was attempted further. The TMS group can be removed and transformed into bromide **3b**. Coupling between **3b** and **2c** in the presence of a catalytic amount of palladium complex furnished trimethylsilylated quaterthiophene ester **4a** in overall 70% yield from **3a**. The same bromination−Stille coupling reaction sequence was applied to **4a** and the desired sexithiophene **5a** was obtained in overall 55% yield from **4a**. In a similar

Scheme 3

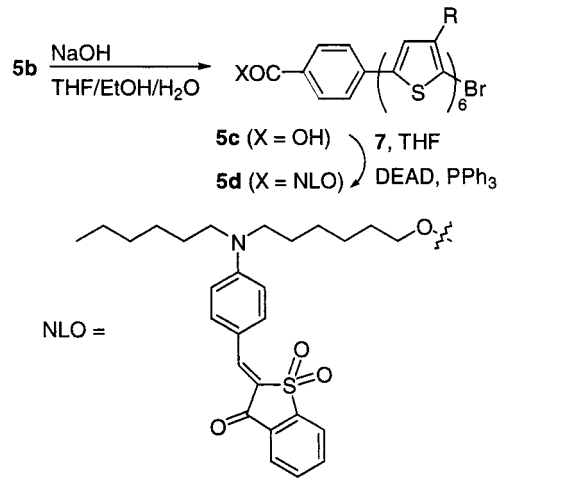

Scheme 4

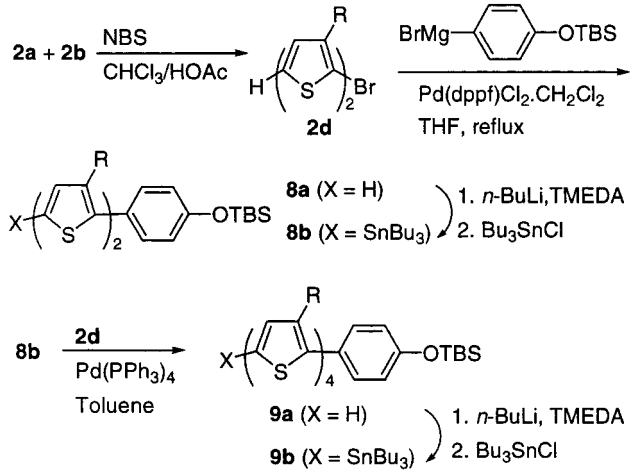

fashion, octithiophene **6a** capped with a terminal TMS group was also prepared in overall 50% yield from **5a**. Compound **5b** can be cleanly converted to acid **5c,** which was immediately condensed with NLO chromophore **7** under the Mitsunobu condition to provide sexithiophene **5d** bearing a NLO chromophore in overall 70% yield from **5b** (Scheme 3).

To prepare the complementary OT series, bromobithiophene **2d** was synthesized in a moderate yield (60%) from a mixture of **2a** and **2b** (NBS, $CHCl_3$−HOAc) (Scheme 4). A Kumada coupling[41] between **2d** and the Grignard reagent derived from 4-[(*tert*-butyldimethylsilyl)oxy]bromobenzene provided the corresponding bithiophene **8a** in 70% yield (Scheme 4). The same Grignard reagent was stannylated and cross-coupled with **5d** to give sexithiophene **10** (60%). Elongation of **8a** was readily achieved by a lithiation−stannylation sequence followed by Stille coupling with **2d** to furnish quaterthiophene **9a** in 65% yield. Assembly of the two complementary OT series was implemented by the Stille coupling of **5d** with tributylstannylated bithiophene **8b** to provide phenyl-capped octithiophene **11**. In a similar fashion, fully functionalized decithiophene **12** was accessible by cross-coupling **5d** with quaterthiophene organostannane **9b** (Scheme 5).

(41) Tamao, K.; Kodama, S.; Nakajima, I.; Kumada, M. *Tetrahedron* **1982**, *38*, 3347.

Scheme 5

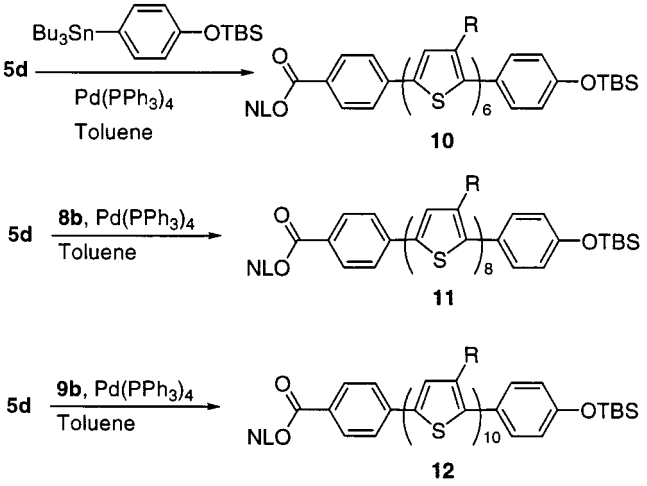

Thermal Properties. All of the functionalized oligothiophene molecules containing NLO chromophore were obtained as amorphous soft red solids and exhibit excellent solubility in a variety of organic solvents such as hexanes, toluene, chloroform, and THF. It was found that all the purified compounds were stable under ambient conditions and were able to sustain a shelf life of more than 1 year. Thus, optical films made of these materials can be maintained in the amorphous state for a long time without noticeable degradation. Differential scanning calorimetry (DSC) studies showed low glass transition temperatures: $T_g = -3.2$, -2.6, and -1.8 °C for **10**, **11**, and **12**, respectively. These low T_g values originates from the large number density of the branched alkyl side chains on the thiophene rings, effectively preventing the bulk materials from crystallization. The low-T_g characteristics enhance the PR performance of these materials through reorientation of the dipolar NLO chromophore in response to a photoinduced space-charge field (orientational enhancement effect).[42]

Optical Properties. The optical properties of the trimethylsilyl-terminated OT esters **3a**−**6a** and the fully functionalized molecules **10**−**12** were studied by UV−vis absorption spectroscopy. For the trimethylsilylated OT series, broad and featureless absorption bands that can be ascribed to the $\pi-\pi^*$ transition of the conjugated oligothiophene backbone are observed (Figure 1). This transition shows a red shifting from $\lambda_{max} = 367$ nm for bithiophene ester **3a** to 397 nm for quaterthiophene **4a**, to 408 nm for sexithiophene **5a**, and finally to 416 nm for octithiophene **6a** with simultaneous increases in molar absorptivity upon successive addition of a conjugated bithiophene unit. The UV−vis absorption spectra of NLO chromophore **7** and fully functionalized **10**−**12** are shown in Figure 2. The spectrum of **7** consists of an intense absorption band at $\lambda_{max} = 492$ nm, which is assigned to the charge-transfer transition of the dipolar chromophore. The spectra of the oligomers **10**−**12** show two major peaks: an intense lower energy transition band (ca. 490 nm) with a tail extending to ~600 nm, as well as a large shoulder in the higher energy region of 420−440 nm, which is due to the absorption of the conjugated OT backbone. The appearance of the large shoulder is the result of a linear superposition of the absorption of both the conjugated backbone and the NLO chromophore moiety. It is clear that the absorbance of the lower energy band correlates well with the concentration of the NLO chromophore unit. As the conjugation chain length increases, not only does the ratio of backbone to chromophore absorbance increase but also the centers of the shoulder peaks show consecutive red shifts of ~5 nm. The absorption behavior of these functionalized OTs can be considered a linear combination of the individual functional components.

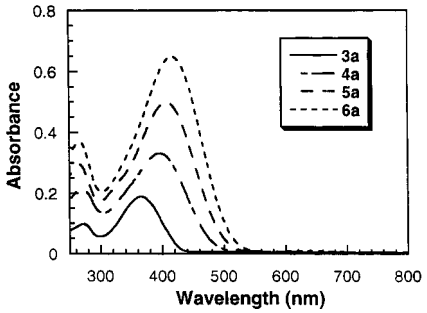

Figure 1. UV−vis absorption spectra of trimethylsilylated oligothiophenes **3a**−**6a** in chloroform ($c = 1 \times 10^{-5}$ mol L^{-1}).

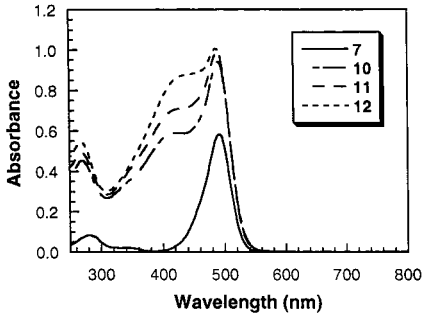

Figure 2. UV−vis absorption spectra of NLO chromophore **7** and fully functionalized oligothiophenes **10**−**12** in chloroform ($c = 1 \times 10^{-5}$ mol L^{-1}).

Table 1. Cyclic Voltammetry Data of NLO Chromophore 7 and Functionalized Oligomers 10−12 in CH_2Cl_2 ($c = 1 \times 10^{-3}$ Mol L^{-1}) with 0.1 Mol L^{-1} Bu_4NPF_6 as the Supporting Electrolyte at a Scan Rate of 100 mV s^{-1}

	oxidation[a]				reduction[a]	
compound	E_{ox1} (V)	E_{ox2} (V)	E_{ox3} (V)	E_{ox4} (V)	E_{red1}[b,c] (V)	E_{red2}[b,c] (V)
7	0.74				−1.54	−2.10
10	0.31	0.44	0.71[b]	0.99[c]	−1.57	−2.38
11	0.30[d]	0.36[d]	0.71[b]	0.84	−1.55	−2.37
12	0.29[d]	0.33[d]	0.55	0.71[b]	−1.55	−2.37

[a] All $E_{1/2}$ values are taken as the average of the anodic and cathodic peak potentials unless otherwise specified and all values are based on the Fc/Fc$^+$ redox couple as internal reference. [b] Redox processes of the NLO moiety. [c] Irreversible redox process and $E_{1/2}$ estimated from $i = 0.8517 i_p$.[26] [d] Difficult to determine as a result of overlapping of the E_{ox1} and E_{ox2} oxidation waves, $E_{1/2}$ estimated from $i = 0.8517 i_p$.[26]

Redox Properties. The electrochemistry of **7** and oligomers **10**−**12** was studied by using a cyclic voltammetric method (Table 1). The NLO chromophore **7** showed a reversible one-electron oxidation process at +0.74 V (vs Fc/Fc$^+$), as well as two irreversible reduction processes at −1.54 V and −2.10 V (vs Fc/Fc$^+$). For the functionalized oligomers **10**−**12**, electrochemical response due to both the NLO moiety and the OT backbone were observed. In general, the oxidation

(42) Moerner, W. E.; Silence, S. M.; Hache, F.; Bjorklund, G. C. *J. Opt. Soc. Am. B* **1994**, *11*, 320.

Table 2. Selected Photorefractive Data of Oligomers 10−12 at a Light Wavelength of 632.8 nm and Applied Field of 78 V μm^{-1}

	oligomers[a]		
	10	**11**	**12**
α^b (cm^{-1})	9.74	10.3	25.7
$\Gamma_p{}^c$ (cm^{-1})	76.9	94.7	30.7
Φ^d (deg)	78	88	72
$\eta_p{}^e$ (%)	18.9	25.1	10.0
$\Delta n^{fi}(10-4)^f$	8.06	7.57	4.02
$\Delta n^{sc}(10-4)^g$	8.07	9.40	4.32
$r_n{}^h$	1.00	1.24	1.17

[a] All PR data were determined at a light wavelength of 632.8 nm and applied field of 78 V μm^{-1}. [b] α is absorption coefficient. [c] Γ_p is the PR gain coefficient for two *p*-polarized beam coupling. [d] Φ is the phase shift between the index and the intensity gratings. [e] η_p is the diffraction efficiency for a *p*-polarized light. [f] Δn^{fi} is the applied field induced birefringence. [g] Δn^{sc} is the index modulation by the space-charge field. [h] r_n is defined as $\Delta n^{sc}/\Delta n^{fi}$ (see text).

potential of the OT backbone decreases with increasing conjugation length of the oligomers. The CV results for sexithiophene **10** indicated four oxidation processes together with two irreversible reduction processes assignable to the chromophore reduction. The first two oxidation waves at +0.31 and +0.44 V (vs Fc/Fc^+) are OT backbone oxidation processes. The third redox transition at +0.71 V for **10** corresponds to the oxidation of the NLO moiety based on the value observed for chromophore **7**. The two irreversible reduction processes, assignable to the reduction of the NLO moiety, are cathodically shifted to −1.57 and −2.38 V (vs Fc/Fc^+) compared to chromophore **7**. As the chain length increases, the determination of the first two oxidation potentials for oligomers **11** and **12** was complicated by overlapping of the two redox waves corresponding to their first and second oxidation processes. Nevertheless, the first and second oxidation potentials for **11** were cathodically shifted to +0.30 and +0.36 V (vs Fc/Fc^+), respectively, while the peak at +0.71 V (oxidation of the NLO moiety) remained virtually unchanged compared to oligomer **10**. Two irreversible reduction waves were also observed at −1.55 and −2.37 V. For the longest oligomer **12**, due to the more extended conjugation of the OT backbone, the first, second and third oxidation potentials further decreased to +0.29, +0.33, and +0.55 V (vs Fc/Fc^+), respectively, while the oxidation (+0.71 V) and reduction (−1.55 and −2.37 V) potentials of the NLO moiety remained essentially unchanged compared to oligomer **11**. The invariance of the redox potentials for the NLO moiety throughout the oligomer series suggests that there is no significant contribution of the NLO chromophore to the observed decrease in oxidation potentials of the OT units.

Photorefractive Properties. Because of the amorphous nature of the materials, high-quality transparent thick films can be conveniently cast from solution. Their photorefractive properties were determined by two-beam coupling and degenerate four-wave mixing (DFWM) experiments and the results are summarized in Table 2. The photorefractive nature of these materials is demonstrated by the observation of clear asymmetric energy exchange (two-beam coupling) between the two incident writing beams: one beam gained energy and the other lost energy. The two-beam coupling gain coefficient (Γ) was calculated according to[1]

$$\Gamma = \frac{1}{L}\ln\left(\frac{1+\alpha}{1-\beta\alpha}\right) \quad (1)$$

where α is the intensity modulation of the signal beam, β is the intensity ratio of the two incident writing laser beams, and L is the optical path length of the beam with gain.

Of the three PR molecular materials examined, the highest PR optical gain coefficient ($\Gamma = 94.7\ cm^{-1}$) was achieved with octithiophene **11** at an applied field of 78 V μm^{-1} and a wavelength of 632.8 nm. This result corresponds to a net optical gain of 84.4 cm^{-1} as the gain exceeds the absorption coefficient ($\alpha = 10.3\ cm^{-1}$). This value is similar to that in our previously reported photorefractive oligothiophene system[13] in which a net gain of 83 cm^{-1} was obtained at $E = 70.6$ V μm^{-1}. The similarity in the PR performance between these two structurally similar oligothiophene-based systems indicates that the conjugation of the OT backbone and NLO moieties does not significantly improve the efficiency of these molecules. This is possibly due to the saturation of the conjugation length of the OT system and also the limited number of NLO moieties incorporated into the molecules. Efforts to extend the effective conjugation length and to increase the NLO chromophore density in these systems will be the subject of future investigations. Nevertheless, it is believed that index modulation benefits greatly from the high orientational (rotational) mobility of the NLO chromophore in response to the local electric field due to the orientational enhancement effect, as commonly observed in other amorphous low-T_g organic PR polymers.[2−4,42] It was observed that as the electric field was switched off, the two-beam coupling gain and loss signals disappeared and their original intensities were restored. Also, a complete erasure and rewriting of the grating could be performed with good reversibility and reproducibility.

As expected, sizable optical gains were also observed for the other two oligomers in this series: $\Gamma = 76.9$ and 30.7 cm^{-1} for sexithiophene **10** and decithiophene **12**, respectively. These yield net two-beam coupling gain of 67.2 and 5.0 cm^{-1} for the two oligomers at an applied field of 78 V μm^{-1} (the absorption coefficients are 9.74 and 25.7 cm^{-1}, respectively). The dependence of two-beam coupling gain for oligomers **10**−**12** on the applied electric field follows a superlinear behavior typical of most PR systems (Figure 3). As the electric field increases, the gain initially increases slowly and then rapidly increases to a maximum value limited by the accessible applied field. The phase shift of the index grating with respect to the intensity grating (illumination pattern) was observed to increase with the applied field and was determined to be 78°, 88°, and 72° for the oligomers **10**−**12**, respectively at the highest applied field of 78 V μm^{-1}, indicating a nonlocal nature of the index grating. The variation of phase shift with the applied electric field for sexithiophene **10** is shown in Figure 4.

Degenerate four-wave mixing experiments were performed to yield further information on the PR properties of the oligomers. The influence of conjugation chain length on the diffraction efficiency follows a trend similar to that of PR optical gain. The decithiophene **12** associated with the longest chain length shows a smaller diffraction efficiency (10.0%) than that of either

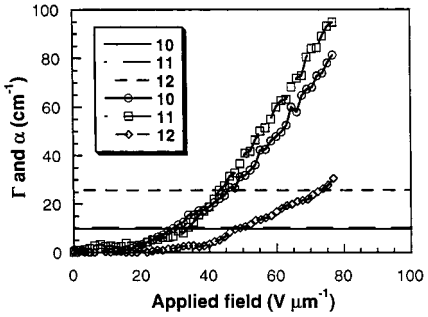

Figure 3. PR two-beam coupling gain and absorption coefficients for oligomers **10**−**12** as a function of applied field.

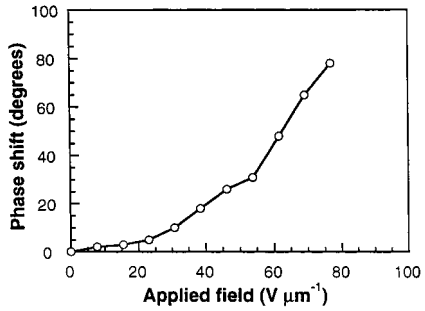

Figure 4. Phase shift of the index grating with respect to the intensity grating for functionalized oligomer **10**.

sexithiophene (18.9%) or octithiophene (25.1%) at a field of 78 V μm^{-1}. The diffraction efficiency increases superlinearly with increasing applied field. This trend in the change of both the diffraction efficiency and PR gain of the oligomers upon increasing chain length suggests that the same photorefractive effect is responsible for both the asymmetric energy exchange in two-beam coupling experiment and diffraction of the reading beam in DFWM experiment.

This dependence of PR properties on conjugation length is interesting and is related to the space-charge field formation process and the NLO chromophore density. Since the NLO moiety is responsible for the absorption tail extended into the 632.8 nm peak, the photocharge generation process occurs mainly at the NLO chromophore rather than at the OT backbone. As the oxidation potentials of the OT backbone is significantly lower than that of the NLO chromophore throughout the oligomer series (Table 1), holes will preferentially migrate from the chromophore site to the OT backbone. As the conjugation length increases, the backbone oxidation potential decreases and the charge-transfer rate from the NLO moiety to the OT unit increases, leading to an improvement in the efficiency of photogeneration process. Thus, an increase in photocharge generation efficiency and enhancement of the space-charge field is expected upon lengthening the oligothiophene chain from sexithiophene **10** to decithiophene **12**. Also of importance is the possible change in number density of the trapping sites as the number of thiophene rings changes; however, its influence on the space-charge field is difficult to predict because there is uncertainty as to the exact nature and distribution of the trapping sites. On the other hand, the number density of NLO chromophore was reduced, as the oligomers become longer, resulting in a retardation of the index modulation. On the basis of these considerations, it can be envisaged that the initial increase in PR optical gain and diffraction efficiency from the sexi- to octithiophene materials could be mainly attributed to the enhancement in space-charge field, as a result of an increase in photogeneration efficiency. On the contrary, as the number of thiophene rings changes from eight to ten, the decreasing NLO chromophore density results in a reduction of index modulation and leads to diminished optical gain and diffraction efficiency.

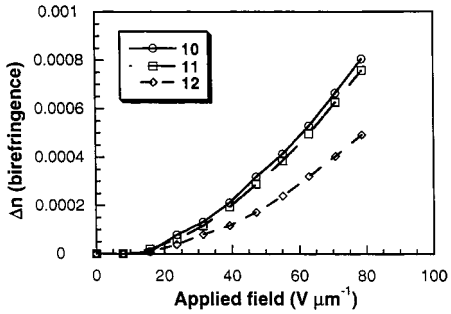

Figure 5. Field-induced birefringence of oligomers **10**−**12** as a function of applied field.

To further elucidate this interesting relationship, the field-induced birefringence was also determined with an ellipsometric method.[28,29] The applied field dependence of Δn^{fi} is shown in Figure 5. The birefringence shows a field enhancement behavior and Δn^{fi} values of 8.06×10^{-4}, 7.57×10^{-4}, and 4.02×10^{-4} at an applied field of 78 V μm^{-1} for oligomers **10**−**12**, respectively. In our oligothiophene PR system, the birefringence is mainly caused by the orientational modulation of the NLO chromophore in response to an external field, while contribution of the linear electrooptic effect is relatively small. The space-charge field induced index modulations Δn^{sc} were also determined according to

$$\eta_p = \sin^2\left(\frac{\pi \Delta n^{sc} L \cos 2\theta_0}{\lambda(\cos\theta_1 \cos\theta_2)^{1/2}}\right) \qquad (2)$$

where L is the optical path in the film, θ_0 is the full angle between the writing beams, λ is the light wavelength, and θ_1 and θ_2 are the reading and the diffracted beam internal propagation angles in the film. The index modulation Δn^{sc} also shows a superlinear dependence on the applied field.

To compare the strength of the space-charge field among the three materials under the same applied field and geometric conditions, it is necessary to normalize the contribution of the number density of the NLO chromophore for the three oligomers. Our normalization procedure is the following. Since both Δn^{fi} and Δn^{sc} are proportional to the number density of the NLO chromophore, the ratio $r_n = \Delta n^{sc}/\Delta n^{fi}$ excludes the influence of the NLO chromophore density for the three oligomers if the external field in all the experiments are the same. To correlate the experimental r_n values with the molecular properties in the microscopic level, the oriented gas model[43] is applied to the low-T_g materials, and the index modulation Δn^{sc} of the PR gratings is given by[42,44]

(43) Wu, J. W. *J. Opt. Soc. Am. B* **1991**, *8*, 142.
(44) Kippelen, B.; Meerholz, K.; Peyghambarian, N. In *Nonlinear Optics of Organic Molecules and Polymers*; Nalwa, H. S.; Miyata, S., Eds.; CRC Press: Boca Raton, FL, 1997.

$$\Delta n^{sc} = \frac{2\pi}{n} C_{BR} G_{BR} E_{ext} E_{sc} + \frac{8\pi}{n} C_{EO} G_{EO} E_{ext} E_{sc} \quad (3)$$

with

$$C_{BR} = \frac{2}{45} N f_\infty \Delta\alpha \left(\frac{\mu^*}{k_B T}\right)^2 \qquad C_{EO} = \frac{N f_0 N f_\infty \beta \mu^*}{15 k_B T} \quad (4)$$

where N is the number density of chromophore, $f_\infty = (n^2 + 2)/3$, $f_0 = \epsilon(n^2 + 2)/(n^2 + 2\epsilon)$, E_{ext} is the external applied field, n is the refractive index, ϵ is the static dielectric constant of the materials, $\Delta\alpha$ is the polarizability anisotropy, β is the first hyperpolarizability of the NLO chromophore, μ^* is the effective dipole moment, k_B is Boltzmann's constant, and T is the absolute temperature. The G_{BR} and G_{EO} values depend on the experimental geometry and the polarization of the probe beam. On the other hand, the birefringence as determined by ellipsometric method is given by

$$\Delta n^{fi} = \frac{3\pi}{n} C_{BR} E_{ext}^{\ 2} + \frac{8\pi}{n} C_{EO} E_{ext}^{\ 2} \quad (5)$$

Therefore

$$r_n = \frac{\Delta n^{sc}}{\Delta n^{fi}} = \frac{2C_{BR} G_{BR} + 8C_{EO} G_{EO}}{3C_{BR} + 8C_{EO}} r_E \quad (6)$$

where $r_E = E_{SC}/E_{ext}$ is the ratio of the magnitude of the space-charge field to the externally applied field. Since both C_{BR} and C_{EO} are proportional to the number density of the NLO chromophore (eq 4), the parameter r_n defined in this manner eliminates the effect of the NLO chromophore. The variation of r_n as a function of the number of thiophene rings in the oligomers **10**−**12** is shown in Table 2. The initial increase in r_n contributes markedly to the increase in PR gain and diffraction efficiency, despite the slight decrease in birefringence Δn^{fi} going from **10** to **11**. On the other hand, as the number of thiophene rings further increases from eight to ten, both terms Δn^{sc} and Δn^{fi} drop substantially, as a result of the decreasing NLO chromophore density (Table 2). However, one also notes that although both index modulations Δn^{sc} and Δn^{fi} decrease by 47% and 54%, respectively, the change of the r_n value between **11** and **12** is only 6%, which is within the experimental error. The change in PR properties between oligomers **11** and **12** is attributable mainly to the decrease in the NLO chromophore density.

Conclusions

The synthetic approach to a homologous series of fully functionalized regioregular head-to-tail coupled oligo(3-alkylthiophenes) bearing pendant nonlinear optical chromophore has been developed. This approach permits efficient construction of the oligomers via an alternating sequence of bromination and Stille cross-coupling reactions by use of a regiochemically pure bithiophene as the building block. The optical and electrochemical properties of the oligomer series correlates with the conjugation chain length. The birefringence associated with the novel NLO chromophore in these low-T_g materials is exploited to optimize the PR performance. Reasonably large net optical gain and diffraction efficiency was achieved in these molecular PR materials. Interesting dependence of the PR performances on the conjugation length of the oligomers was observed. It was rationalized that the better performance of **11** over that of **10** is mainly due to the enhancement of the space-charge field, while decrease in number density of the NLO chromophore is responsible for the difference between **11** and **12**.

Acknowledgment. This work was supported by the National Science Foundation and the Air Force of Scientific Research. Support from the National Science Foundation Young Investigator program is gratefully acknowledged. This work also benefited from the support of NSF MERSEC program at the University of Chicago.

Supporting Information Available: Experimental procedures for synthesis of compounds **1a**−**c**, **2a**, **2d**, **3a**, **3b**, **4a**, **4b**, **5a**, **5d**, **6a**, **8a**, **8b**, **9a**, and **9b**. This material is available free of charge via the Internet at http://pubs.acs.org.

CM000232X